Supplementary Information for

Glycine/PVP-Enabled One-Pot CRISPR/Cas13a Detection of *Vibrio parahaemolyticus* by Tetrahedron-mediated Electrochemistry

Jincheng Zhang[1,2†], Shuang Liang[1,2 †], Yue Sun[2], Cuixing Zhan[2], Gan Xue[2], Xin Zhou[1*]

1. The First Hospital of Hebei Medical University, Shijiazhuang 050000, China

2. College of Veterinary Medicine, Institute of Comparative Medicine, Yangzhou University, Yangzhou 225009, China

† These authors contributed equally to this work.

Experimental Section

Reagents and Instruments

Recombinase-aided amplification (RAA) basic kits and the Genchek isothermal fluorescence amplification instrument were purchased from Hangzhou ZC Bio-Sci & Tech. (Hangzhou, China). The T7 High Yield Transcription Kit was obtained from Yeasen Biotechnology (Shanghai, China). XbaI was purchased from New England Biolabs (NEB, USA). The pMD18-T cloning vector and DNA Ligation Kit were purchased from Takara Bio Inc. (Shiga, Japan). 2× SYBR Green Master Mix and 2× Phanta Max Master Mix were purchased from Vazyme Biotech Co., Ltd. (Nanjing, China). The Gen^{TM} CRISPR Cas13a (C2c2) nuclease was obtained from GenScript (Nanjing, China). Nucleic acid release reagent was purchased from Mole Bioscience (Taizhou, China). Glycine was purchased from Beyotime Biotechnology (Shanghai, China), and polyvinylpyrrolidone (PVP, 10 kDa) was obtained from Merck (Darmstadt, Germany). Gold electrodes were purchased from Changsha Sunjeen Electronic Technology Co., Ltd. (Changsha, China). Anti-FAM13B rabbit polyclonal antibody, Spin Column RNA Cleanup & Concentration Kit and all oligonucleotides (including modified sequence) were synthesized by Sangon Biotech (Shanghai, China). Streptavidin was purchased from Thermo Fisher Scientific (USA), and goat anti-rabbit IgG was obtained from Solarbio (Beijing, China). Chemically competent *Escherichia coli* DH5α cells was purchased from ToloBio (Shanghai, China).

Bacterial Strains and Culture Conditions

Vibrio parahaemolyticus VP17802, *Vibrio alginolyticus* Va2225, *Vibrio vulnificus* Vv-1, *Salmonella* C5004, and *Escherichia coli* ER2738 were preserved in our laboratory collection. All *Vibrio* strains were cultured in alkaline peptone water (APW), whereas non-*Vibrio* strains were cultured in Luria–Bertani (LB) medium.

Preparation of VPA1585 Plasmid Standards and qPCR Analysis

The gene *VPA1585*, a recently identified and reported species-specific marker of *Vibrio parahaemolyticus*, was selected as the molecular target for pathogen detection in this study[1]. Compared with commonly used target genes, including the virulence-associated genes *tdh*, *trh*, and *tlh*, as well as housekeeping genes such as *toxR*, *gyrB*, and *flaE*, these conventional targets may be undetectable in certain strains or yield false-negative results, thereby compromising diagnostic accuracy[2,3]. A 489 bp fragment of the *VPA1585* gene was amplified using primers VPA1585-Fw and VPA1585-Rv from *Vibrio parahaemolyticus* VP17802 (Table S1) and cloned into the pMD18-T vector *via*

TA cloning to generate a plasmid standard for construction of the qPCR standard curve. As a gold-standard reference method, qPCR was conducted using 10-fold serial dilutions of the plasmid standard to benchmark the performance of the proposed assay. Each 20 μL reaction contained 10 μL of 2× SYBR Green Master Mix (Vazyme, China), 0.4 μL each of qVPA1585-Fw and qVPA1585-Rv primers (10 μM，Table S1), 1 μL of template DNA, and nuclease-free water. The qPCR cycling program was 95 °C for 30 s, followed by 40 cycles of 95 °C for 10 s and 60 °C for 30 s. Melt curve analysis was used to confirm specificity.

Recombinase-Aided Amplification (RAA)

RAA primers targeting the *VPA1585* gene were designed using Oligo 7 and Primer-BLAST, with a T7 promoter sequence appended to the 5′ end of the forward primer for subsequent *in vitro* transcription. RAA reactions were performed according to the manufacturer's instructions. Briefly, each 50 μL reaction contained one lyophilized enzyme pellet, 25 μL of Buffer A, 2 μL of RAA primers (10 μM each), 13.5 μL of nuclease-free water, and 5 μL of DNA template, with 2.5 μL of Buffer B added to initiate the reaction. To establish the optimal amplification conditions, key parameters including primer sequence, reaction time, reaction temperature, and analytical sensitivity were systematically evaluated. Amplification products were analyzed by 2% agarose gel electrophoresis and visualized using Bio-Rad gel imaging system, and band intensities were quantified using ImageJ software for semi-quantitative assessment of amplification efficiency. Primer sequences are provided in Table S2.

Design and Preparation of crRNA by *In Vitro* Transcription

crRNA sequences and corresponding DNA templates were designed using SnapGene software and verified for specificity using the NCBI BLAST online tool. Single-stranded DNA oligonucleotides containing the T7 promoter and crRNA sequence were synthesized and annealed to form double-stranded DNA fragments, which were subsequently cloned into the pMD18-T vector using a standard TA cloning procedure. crRNA sequences were designed using SnapGene and verified by BLAST. DNA templates containing the T7 promoter and crRNA sequence were synthesized, cloned into the pMD18-T vector, and linearized with XbaI. *In vitro* transcription was performed using a T7 High Yield Transcription Kit according to the manufacturer's protocol. The resulting crRNAs were purified using an RNA Clean & Concentrator Kit

(Sangon Biotech, China), quantified by NanoDrop, and stored at −80 °C until use. crRNA sequences are provided in Table S2.

Establishment and Optimization of the Glycine/PVP-Enabled One-pot CRISPR Framework

To improve assay sensitivity and decouple the effects of RAA from CRISPR signal generation, a two-step workflow was first established. In this format, RAA amplification and IVT–CRISPR/Cas13a detection were performed sequentially in separate reactions, whereas the one-pot format integrates RAA, transcription, and Cas13a collateral cleavage in a single isothermal system. RAA was performed under the optimized conditions described. Then, 5 μL of the RAA product was introduced into a 45 μL IVT–CRISPR/Cas13a reaction containing 5 μL 10× Transcription Buffer (400mM Tris-HCl, 460mM $MgCl_2$, 20 mM spermidine, 100mM DTT), 2 μL T7 RNA Polymerase Mix, 8 μL rNTP mixture (100 mM), 5 μL 10× Cas13a Reaction buffer (400mM Tris-HCl, 600mM $NaCl_2$, 60mM $MgCl_2$), 1 μL Cas13a protein, 1 μL crRNA, and 1 μL ssRNA reporter, supplemented with DEPC-treated water. Reactions were conducted at 37 °C and monitored by real-time fluorescence. Key parameters including crRNA sequence, crRNA concentration, Cas13a concentration, reporter concentration, T7 polymerase concentration, and rNTP concentration were systematically optimized.

To facilitate practical operation and minimize contamination risk, the optimized two-step workflow was adapted to establish a one-pot format, in which RAA amplification, T7-mediated *in vitro* transcription, and Cas13a-mediated collateral cleavage were performed simultaneously in a single tube. Glycine (20%, 15%, 10%, 5%, and 1%) and polyvinylpyrrolidone (PVP, 10 kDa; 10%, 5%, 2%, 1%, and 0.5%) were individually introduced into the reaction system, and their concentrations were systematically optimized for the one-pot RAA–CRISPR/Cas13a assay using standard plasmid DNA at a final concentration of 3×10^1 copies μL^{-1}. The optimal concentration of each single additive was then selected for evaluation of their combined effect using standard plasmid DNA at a final concentration of 3 copies μL^{-1}.To further assess the influence of common matrix components on the regulatory effects of glycine and PVP, standard plasmid DNA was spiked into buffer, 3% NaCl alkaline peptone water (3% NaCl APW), pond water, and healthy shrimp tissue matrices to a final concentration of 3×10^1 copies μL^{-1}, followed by analysis using the established one-pot RAA–CRISPR/Cas13a fluorescence assay. A premixed solution was prepared containing 10

μL of 10× Transcription Buffer, 10 μL of 10× Cas13a Reaction Buffer, 25 μL of Buffer A, Cas13a protein, T7 RNA Polymerase Mix, ssRNA fluorescent reporter probe, rNTP mixture, RAA primers, crRNA, Glycine, PVP and DEPC-treated water. This premix was used to resuspend the lyophilized RAA enzyme pellet, forming the complete reaction system. Each reaction was initiated by adding 2 μL of DNA template (pMD18-T-VPA1585 plasmid standard) and 2.5 μL of Buffer B, resulting in a final reaction volume of 100 μL. The reaction was conducted at 37 °C with real-time fluorescence monitoring using the isothermal fluorescence detection instrument. All optimization experiments were performed by varying a single parameter while keeping the remaining components constant.

TD-Mediated the Glycine/PVP-Enabled One-pot CRISPR Framework Electrochemical Detection

TD sequence and the positions of uracil incorporation that enable Cas13a-responsive cleavage are provided in Table S3 [4], and TD nanostructures were assembled following a reported protocol with minor modifications[5]. Thiol-modified and unmodified oligonucleotides were dissolved in nuclease-free water to a final concentration of 10 μM and mixed thoroughly. TD assembly was performed in phosphate-buffered saline (PBS) containing 5 mM Mg^{2+} and 1 mM tris(2-carboxyethyl)phosphine hydrochloride (TCEP·HCl). To verify stepwise assembly, different strand combinations (S1-SH; S1-SH + S2-SH; S1-SH + S2-SH + S3; and S1-SH + S2-SH + S3 + S4-SH) were prepared. The mixtures were heated to 95 °C and slowly cooled to room temperature, followed by incubation at 4 °C for 1 h to complete TD formation.

TD assembly was characterized by native polyacrylamide gel electrophoresis (PAGE), in which stepwise changes in electrophoretic mobility reflected progressive strand assembly. Cas13a-mediated trans-cleavage of TD was evaluated by incubating TD with Cas13a protein, crRNA, and target RNA, followed by analysis using native PAGE. Dynamic light scattering (DLS Malvern Zetasizer Nano ZS90) was used to determine the hydrodynamic diameter and zeta potential of the TD nanostructures. The structural morphology and conformation of the TD were characterized by TEM (HT7800, Hitachi, Japan).

For electrode functionalization, 10 μL of the assembled TD solution was drop-cast onto a gold electrode (GE) surface and incubated at 4 °C overnight to allow

immobilization via Au–S bonding. After rinsing thoroughly with ultrapure water, the electrode surface was passivated with 1 mM 6-mercapto-1-hexanol (MCH) at room temperature for 1 h to reduce nonspecific adsorption. Subsequently, methylene blue (MB) was loaded onto the TD-modified electrode by incubation with 100 μM MB solution at 37 °C for 30 min. The resulting electrode was denoted as GE@TD-MB@MCH and used for subsequent electrochemical measurements.

For electrochemical sensing, the reaction mixture containing the one-pot CRISPR system (without the ssRNA reporter probe) and target analytes was incubated on the GE@TD-MB@MCH electrode. Electrochemical measurements, including cyclic voltammetry (CV), electrochemical impedance spectroscopy (EIS), and square wave voltammetry (SWV), were performed using a CHI 660C electrochemical workstation under standard operating conditions.

The Glycine/PVP-Enabled One-pot CRISPR Framework Combined with LFA Detection

To enable instrument-free visualization of the glycine/PVP-enabled one-pot CRISPR framework, an LFA readout based on a colloidal gold system was established. In this format, the fluorescence-quenched ssRNA reporter was replaced with a dual-labeled ssRNA reporter probe modified with 5′-FAM and 3′-biotin.

The intact reporter binds to colloidal gold–labeled anti-FAM antibodies and is captured by streptavidin immobilized on the control line. Target-activated Cas13a cleaves the reporter, altering its migration and signal distribution on the strip. For detection, the one-pot CRISPR reaction was conducted using the dual-labeled ssRNA reporter for 30 min, and the dipstick was directly immersed into the reaction mixture. Visual results were obtained within 2 min at room temperature.

Performance Evaluation of the GPT-CRISPR Electrochemical Sensing Platform

The analytical sensitivity of the one-pot CRISPR assay was evaluated using a plasmid standard containing the *VPA1585* gene. The plasmid standard was serially diluted in 10-fold steps from 3×10^0 to 3×10^7 copies μL^{-1} and tested under optimized conditions using fluorescence and LFA readouts. For the GPT-CRISPR electrochemical readout, a separate concentration range (3×10^3–0.38 copies μL^{-1}) was additionally evaluated, considering the enhanced signal transduction capability of the TD-mediated interface. To validate the applicability of the plasmid-derived GPT-CRISPR calibration curve to *Vibrio parahaemolyticus* genomic DNA, V. parahaemolyticus cultures were serially diluted 10-fold and subjected to plate counting, and the bacterial concentrations

were adjusted to 10^0–10^6 CFU/mL. Genomic DNA was then extracted from each dilution and eluted in 50 μL ddH_2O, followed by analysis using both the GPT-CRISPR assay and qPCR to evaluate the agreement between the two methods.

For robustness evaluation of the GPT-CRISPR platform, the influence of common matrix components on the TD-modified interfacial system was assessed by spiking standard plasmid DNA into buffer, 3% NaCl APW, pond water, and healthy shrimp tissue homogenate matrices to a final concentration of 3×10^1 copies μL^{-1}. In addition, the reproducibility of the method was evaluated using six independently prepared TD-based sensors, with standard plasmid DNA at a final concentration of 3×10^1 copies μL^{-1}. Furthermore, to compare the interfacial performance of TD-modified and linear DNA(S1-SH)-modified electrodes, GE@TD-MB@MCH and GE@Linear Nucleic Acid-MB@MCH were constructed and subjected to parallel evaluation of analytical sensitivity and robustness under the same detection conditions. Assay specificity was evaluated using *Vibrio parahaemolyticus* VP17802, *Vibrio alginolyticus* Va2225, *Vibrio vulnificus* Vv-1, *Salmonella* C5004, and *Escherichia coli* ER2738. All samples were analyzed under identical conditions using one-pot CRISPR assay, with specificity independently assessed through fluorescence, LFA, and electrochemical readouts.

Multiscenario Real-Sample Evaluation and Validation

To evaluate the applicability of the proposed detection platform in real-world matrices, a total of 30 samples representing five distinct categories were collected. These included diseased *Litopenaeus vannamei* samples from different aquaculture farm and aquaculture water in Jiangsu Province China, wastewater from seafood markets, double-blind artificially contaminated samples, and chilled salmon samples purchased from supermarkets. Double-blind artificially contaminated samples were prepared in 3% NaCl APW spiked with *Vibrio parahaemolyticus* at 10^0, 10^1, 10^2, and 10^3 CFU/mL. Two unspiked matrix samples served as negative controls. Sample preparation and coding were completed by one researcher, and GPT-CRISPR analysis was performed by a second researcher blinded to sample identity and contamination level. All samples were manually homogenized where applicable and diluted 10-fold using a nucleic acid release reagent. The mixtures were then heated at 95 °C for 5 min for nucleic acid release. The resulting lysates were directly used as templates for the fluorescence-based, LFA, and TD mediated electrochemical GPR-CRISPR assays. The same templates were simultaneously subjected to qPCR analysis, and the detection results obtained using the proposed methods were compared with those from qPCR.

Data Acquisition and Processing

Fluorescence data were collected using an isothermal amplification fluorescence detection instrument and exported for analysis with GraphPad Prism 8. All fluorescence signals in this study were acquired on the same instrument, with a maximum detection plateau of 15,000 relative fluorescence units (RFU, a.u.). Gel electrophoresis images were captured using a gel documentation system.

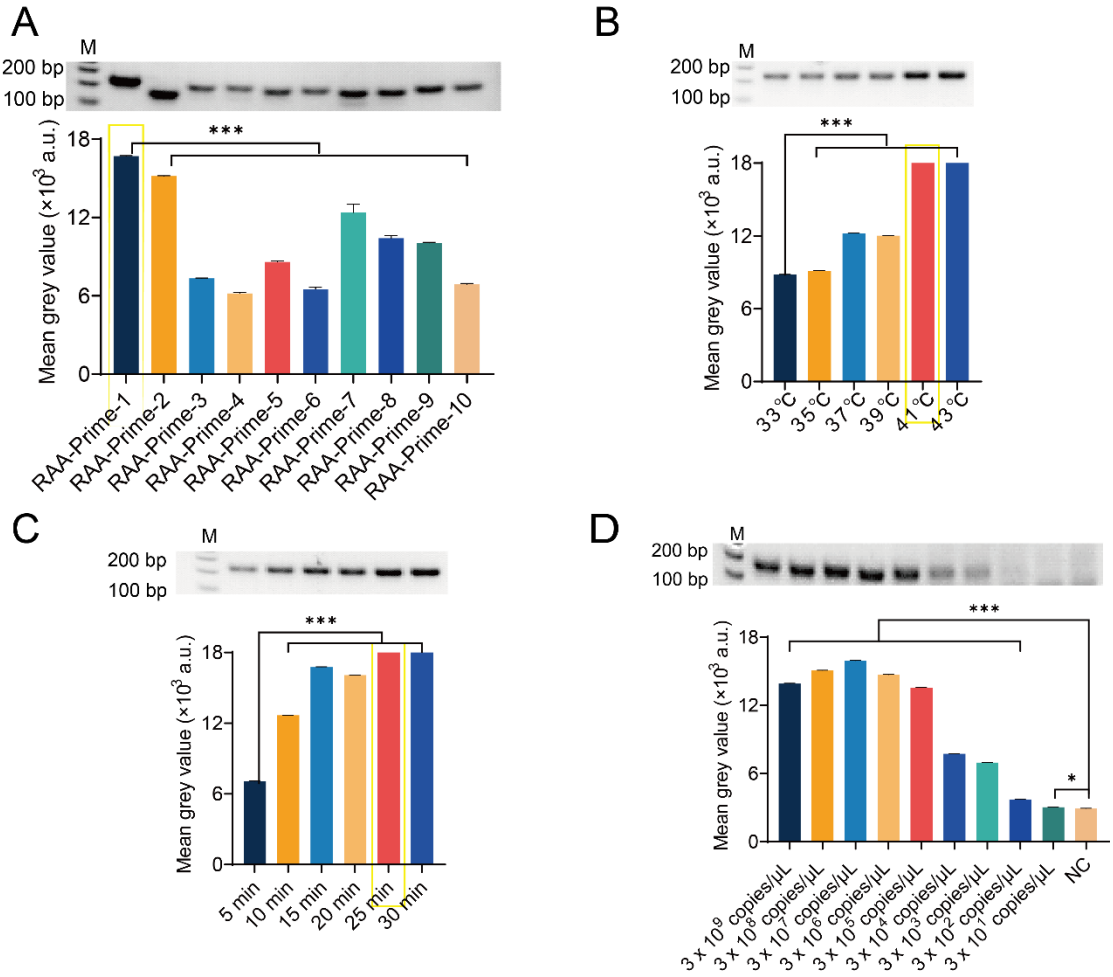


Fig. S1 Optimization of RAA Reaction Conditions. (A) Optimization of RAA primer sequence. (B) Optimization of RAA reaction temperature. (C) Optimization of RAA reaction time. (D) Sensitivity evaluation of the optimized RAA assay using serially diluted DNA templates. For panels (A-D) band intensities were quantified using ImageJ software and are presented as mean grayscale values (± SD). Statistical analysis was performed using one-way ANOVA in GraphPad Prism 8. Significance levels are indicated as ns, $P > 0.05$; * $P \leq 0.05$; ** $P \leq 0.01$; *** $P \leq 0.001$.

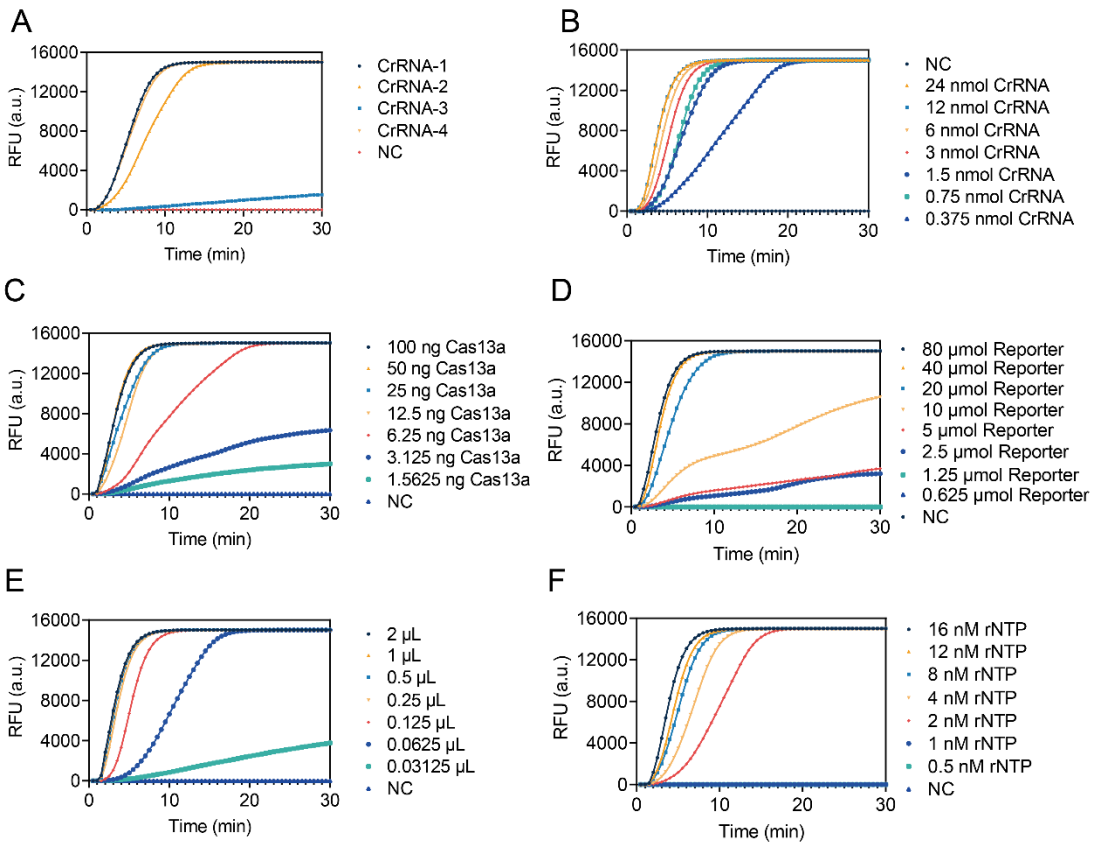


Fig. S2 Optimization of reaction conditions for the CRISPR/Cas13a detection system. (A) Real-time fluorescence kinetics of four candidate crRNAs (crRNA-1 to crRNA-4) evaluated using *in vitro* transcribed RNA targets. (B–F) Optimization of key reaction components affecting CRISPR/Cas13a detection performance, including crRNA concentration (B), Cas13a protein concentration (C), ssRNA reporter concentration (D), T7 RNA polymerase input (E), and rNTP concentration (F). Fluorescence signals were monitored in real time to evaluate cleavage efficiency under each condition.

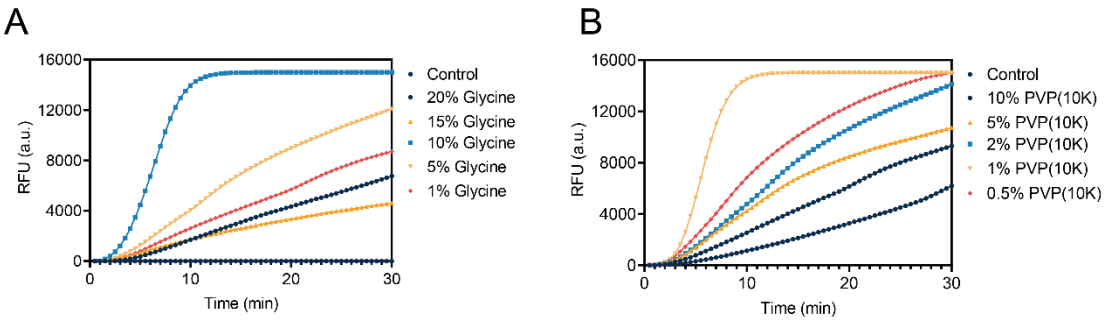


Fig. S3 Effects of glycine and PVP (10 kDa) on the fluorescence kinetics of the one-pot CRISPR reaction. (A) Glycine. (B) PVP (10 kDa).

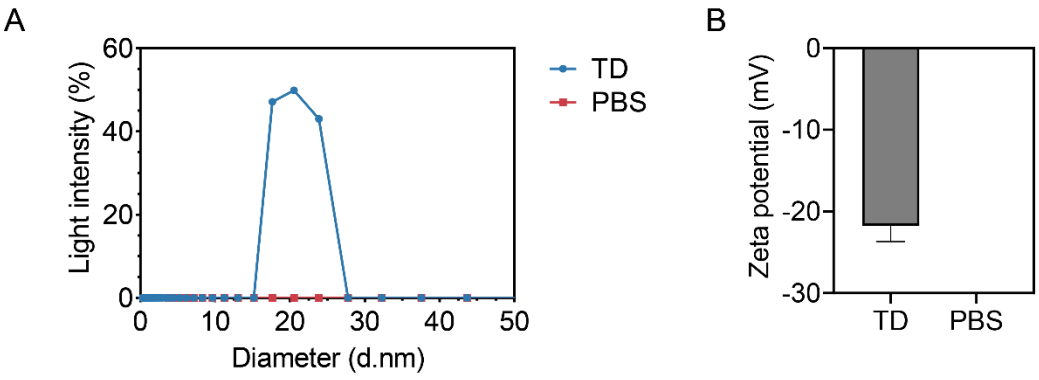


Fig. S4 Characterization of TD nanostructures. (A) Particle size distribution of TD and PBS measured by dynamic light scattering (DLS). (B) Zeta potential measurements of TD and PBS.

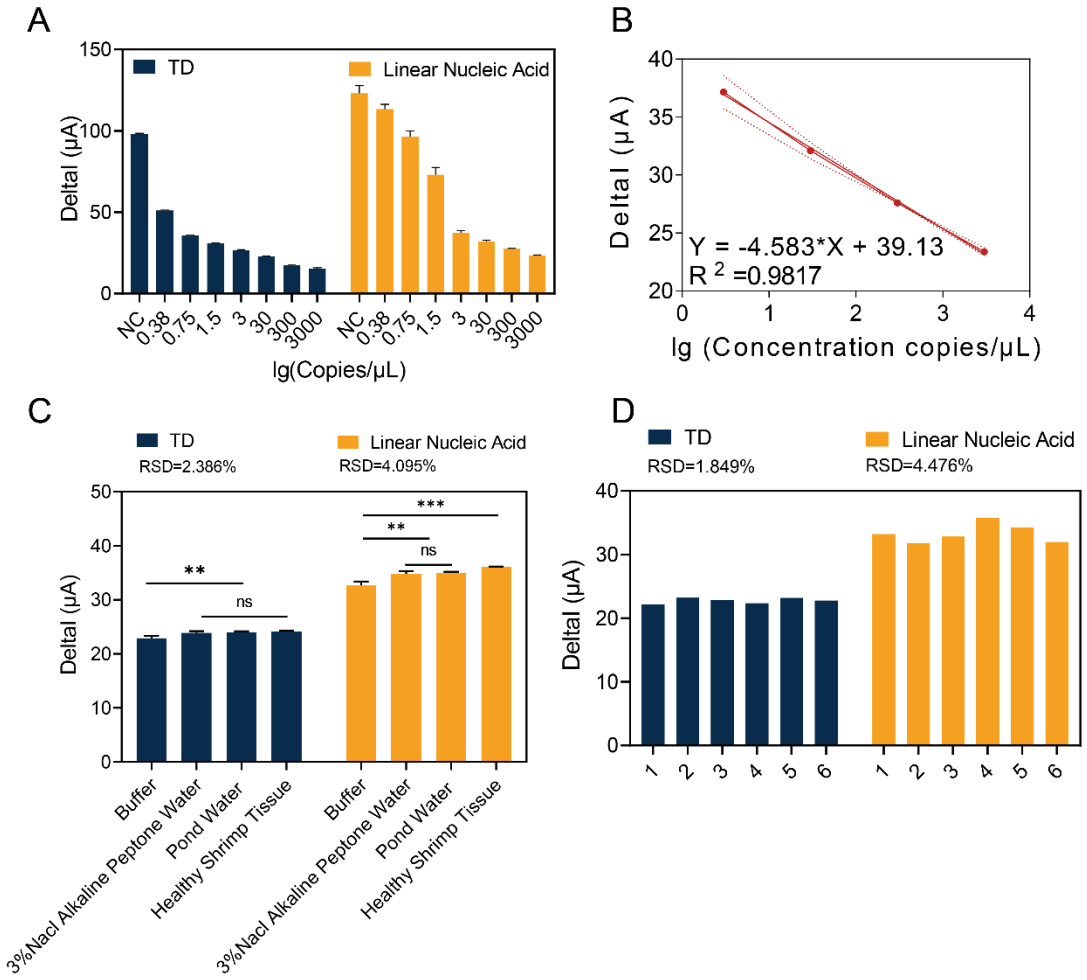


Fig. S5 Comparison of the analytical performance of TD and linear DNA probe interfaces in the GPT-CRISPR platform. (A) Sensitivity comparison of the two interfacial probes. (B) Linear dynamic range of the linear DNA probe-mediated CRISPR assay. (C) Stability of the two interfacial probes in complex matrices. (D) Reproducibility of the two interfacial probes.

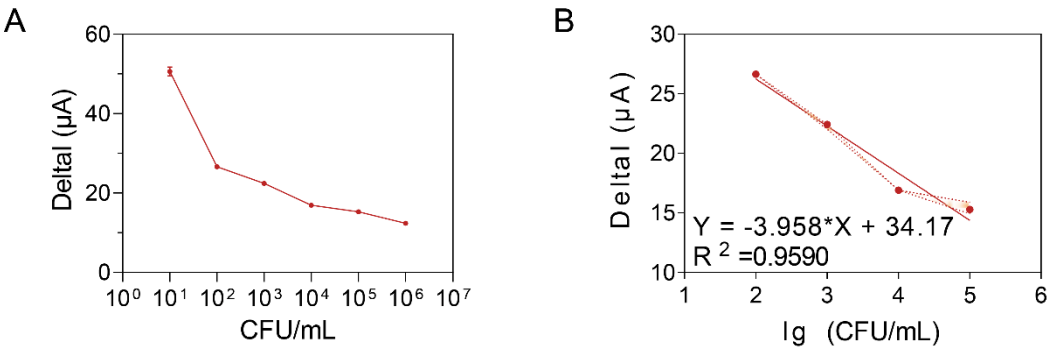


Fig. S6 GPT-CRISPR analysis of genomic DNA extracted from serially diluted *Vibrio parahaemolyticus* cultures. (A) Relationship between *Vibrio parahaemolyticus* concentration (CFU/mL) and the corresponding electrochemical current response. (B) Calibration curve constructed from the electrochemical current response versus the logarithm of *Vibrio parahaemolyticus* concentration.

Table S1. Primer sequences used for qPCR in this study

Name	Sequence (5'-3')
VPA1585-Fw	**ATGTACTCTTCAATTGCGAG**
VPA1585-Rv	**TCAATGTGGCTTTTTTTGAT**
qVPA1585-Fw	**ATGAAAAATGGTCGTGCCGC**
qVPA1585-Rv	**TGCACGACTTTGGTCTTGGT**

Table S2 Sequences used for RAA and CRISPR reactions in this study.

Name	Sequence (5'-3')
RAA1-Fw	***TAATACGACTCACTATA***TGGGTATCAATTTTTGGCTCTATGACTTCCGT
RAA1-Rv	TTCATCACCACTTTGATACCAACAAAACGCAT
RAA2-Fw	***TAATACGACTCACTATA***TATCCCTGCAAGAAAACTTCACGCTTGTTTAC
RAA2-Rv	TTCATCACCACTTTGATACCAACAAAACGCAT
RAA3-Fw	***TAATACGACTCACTATA***TATCCCTGCAAGAAAACTTCACGCTTGTTTAC
RAA3-Rv	TTTCATCACCACTTTGATACCAACAAAACGCA
RAA4-Fw	***TAATACGACTCACTATA***TGGGTATCAATTTTTGGCTCTATGACTTCCGT
RAA4-Rv	TTTCATCACCACTTTGATACCAACAAAACGCA
RAA5-Fw	***TAATACGACTCACTATA***TATCCCTGCAAGAAAACTTCACGCTTGTTTAC
RAA5-Rv	TTGCCCTTCCTTCAACCAATACCAGTTAATCA
RAA6-Fw	***TAATACGACTCACTATA***TATCAATTTTTGGCTCTATGACTTCCGTTTAT
RAA6-Rv	CATTTTTCATCACCACTTTGATACCAACAAAA
RAA7-Fw	***TAATACGACTCACTATA***GTATCAATTTTTGGCTCTATGACTTCCGTTTA
RAA7-Rv	ATTTTTCATCACCACTTTGATACCAACAAAAC
RAA8-Fw	***TAATACGACTCACTATA***ATCAATTTTTGGCTCTATGACTTCCGTTTATC
RAA8-Rv	TTTTTCATCACCACTTTGATACCAACAAAAC

RAA9-Fw	***TAATACGACTCACTATA***TATCAATTTTTGGCTCTATGACTTCCGTTTA
RAA9-Rv	TTCAACCAATACCAGTTAATCACGAGAAGAAT
RAA10-Fw	***TAATACGACTCACTATA***TTTTGTTGGTATCAAAGTGGTGATGAAAAATG
RAA10-Rv	CAGGAATAAACATTTCGAGTAGGTAGCTGATG
CrRNA1	AACAAAACGCATGCCGATGGTTTGCCCT
CrRNA2	GAGAAGAATGGGAACAGTAAGGAGGTAC
CrRNA3	TTCATCACCACTTTGATACCAACAAAAC
CrRNA4	CGGAAGTCATAGAGCCAAAAATTGATAC
ssRNA reporter-1	6-FAM 5‘ -$_{2'\text{-}O\text{-}M}$AAUGGC$_{2'\text{-}O\text{-}M}$A$_{2'\text{-}O\text{-}M}$AAUGGC$_{2'\text{-}O\text{-}M}$A -3’BHQ1
ssRNA reporter-2	6-FAM 5‘ -$_{2'\text{-}O\text{-}M}$AAUGGC$_{2'\text{-}O\text{-}M}$A$_{2'\text{-}O\text{-}M}$AAUGGC$_{2'\text{-}O\text{-}M}$A -3’biotin

Note: Underlined bold italic text indicates the T7 promoter sequence.

Table S3. Sequences used for DNA tetrahedron assembly in this study

Name	**Sequence (5'-3')**
S1-SH	ACATTCCUUUGTCTGAAACATTACAGUUUGCTACACGAGAAGAGCUUUCATAGTA-SH
S2-SH	TATCACCUUUCAGTTGACAGTGTAGCUUUCTGTAATAGATGCGAGUUUCCAATAC-SH
S3	TCAACTGUUUGGTGATAAAACGACACUUUGTGGGAATCTACTATGUUUGCTCTTC
S4-SH	TTCAGACUUUGGAATGTGCTTCCCACUUUGTGTCGTTTGTATTGGUUUCTCGCAT-SH
S1	ACATTCCUUUGTCTGAAACATTACAGUUUGCTACACGAGAAGAGCUUUCATAGTA
S2	TATCACCUUUCAGTTGACAGTGTAGCUUUCTGTAATAGATGCGAGUUUCCAATAC
S4	TTCAGACUUUGGAATGTGCTTCCCACUUUGTGTCGTTTGTATTGGUUUCTCGCAT

Table S4. qPCR Cq values for clinical samples

Sample	Cq value			mean
Sample No.1	24.88	24.67	25.01	24.85
Sample No.2	28.65	28.23	27.99	28.29
Sample No.3	31.78	32.47	32.16	32.14
Sample No.4	17.71	17.52	18.13	17.79
Sample No.5	21.49	21.97	21.54	21.67
Sample No.6	-	-	-	-
Sample No.7	25.16	25.95	25.08	25.40
Sample No.8	17.64	17.37	18.02	17.68
Sample No.9	21.19	21.23	21.54	21.32
Sample No.10	24.89	24.66	25.11	24.89
Sample No.11	28.47	28.52	28.75	28.58
Sample No.12	32.15	32.45	32.22	32.27
Sample No.13	-	-	-	-
Sample No.14	30.69	30.77	30.65	30.70
Sample No.15	17.32	17.43	17.79	17.51
Sample No.16	21.13	21.1	21.65	21.29
Sample No.17	-	-	-	-
Sample No.18	-	-	-	-
Sample No.19	17.68	17.7	17.53	17.64
Sample No.20	-	-	-	-
Sample No.21	21.56	21.79	21.35	21.57
Sample No.22	36.63	36.81	35.22	36.22
Sample No.23	33.79	33.43	33.64	33.62
Sample No.24	36.63	35.74	35.61	35.99
Sample No.25	35.84	35.03	35.84	35.57
Sample No.26	35.12	36.23	35.96	35.77
Sample No.27	33.79	33.22	33.1	33.37
Sample No.28	35.23	35.18	35.63	35.35
Sample No.29	-	-	-	-
Sample No.30	35.39	35.25	35.21	35.28

Note: Samples highlighted in blue indicate qPCR-confirmed negative clinical samples.

Table S5. Summary of reported CRISPR-based detection methods for *Vibrio parahaemolyticus*

Detection method	Core components	Readout mode	Detection time	Detection limit	Reference
LAMP–CRISPR/Cas12a assay	LAMP + Cas12a	Fluorescence / UV visual	<30 min	2.5 CFU/mL	[6]
One-pot LAMP–CRISPR/Cas12b assay	LAMP + Cas12b + IMB	Fluorescence / LFA	<4 h	37 CFU/mL	[7]
One-pot RPA–CRISPR/Cas12a microfluidic biosensor	RPA + Cas12a + centrifugal microfluidics	Microfluidic fluorescence	<1.5 h	6.08 copies/μL	[8]
Dual-channel LAMP–CRISPR/Cas12a biosensor	LAMP + Cas12a + DNA nanoclusters	Colorimetric / ratiometric fluorescence	~2 h	1 CFU/mL	[9]
RPA-mediated electrochemical CRISPR/Cas12a biosensor	RPA + Cas12a + electrochemistry	Electrochemical	~1 h	32 CFU/mL	[10]
Adaptive tandem CRISPR/Cas12a molecular amplifier	RPA + TdT + Cas12a	Fluorescence	NR	12.4 CFU/mL	[11]
CRISPR/Cas14a–Exo III fluorescence biosensor	Aptamer + Exo III + Cas14a	Fluorescence	~1 h	6 CFU/mL	[12]

References

(1) Hu, A.; Kong, L.; Lu, Z.; Qiao, J.; Lv, F.; Meng, F.; Bie, X. Research on nanogold-assisted HRM-qPCR technology for highly sensitive and accurate detection of vibrio parahaemolyticus. *LWT-Food Sci. Technol.* 2022, *162*, 113488, DOI: 10.1016/j.lwt.2022.113488.

(2) Chen, Y.; Chen, X.; Yu, F.; Wu, M.; Wang, R.; Zheng, S.; Han, D.; Yang, Q.; Kong, H.; Zhou, F.; et al. Serology, virulence, antimicrobial susceptibility and molecular characteristics of clinical vibrio parahaemolyticus strains circulating in southeastern china from 2009 to 2013. *Clinical Microbiology and Infection* 2016, *22*(3), 258-259, DOI: 10.1016/j.cmi.2015.11.003.

(3) Hu, A.; Chen, H.; Shi, C.; Lu, Z.; Meng, F.; Bie, X. RT-RPA and RPA-LFA assay for rapid and ultrasensitive detection of vibrio parahaemolyticus. *Food Control* 2024, *166*, 110732, DOI: /10.1016/j.foodcont.2024.110732.

(4) Cheng, L.; Yang, F.; Zhao, Y.; Liu, Z.; Yao, X.; Zhang, J. Tetrahedron supported CRISPR/cas13a cleavage for electrochemical detection of circular RNA in bladder cancer. *Biosens. Bioelectron.* 2023, *222*, 114982, DOI: 10.1016/j.bios.2022.114982.

(5) Zhan, X.; Jiang, Y.; Li, Z.; Hu, X.; Lan, F.; Ying, B.; Wu, Y. Split DNA tetrahedron-mediated spatiotemporal-hierarchy CRISPR cascade integrated with au@pt nanolabels and artificial intelligence for a cervical cancer MicroRNA bioassay. *ACS Nano* 2025, *19*(25), 22849-22869, DOI: 10.1021/acsnano.5c01376.

(6) Hu, A.; Kong, L.; Lu, Z.; Zhou, H.; Bie, X. Construction of a LAMP-CRISPR assay for the detection of vibrio parahaemolyticus. *Food Control* 2023, *149*, 109728, DOI: 10.1016/j.foodcont.2023.109728.

(7) Wang, S.; Gao, Y.; Miao, Y.; Jiang, W.; Zhang, X.; Zheng, Y.; Wang, J.; Zhang, X.; Liao, H.; Li, Y.; et al. Detection of vibrio parahaemolyticus by one-pot LAMP-CRISPR/cas12b combined with immunomagnetic beads. *Food Control* 2025, *172*, 111181, DOI: 10.1016/j.foodcont.2025.111181.

(8) Fang, J.; Chen, Q.; Ran, M.; Chen, R.; Chen, W.; Cui, J.; Wang, J.; Zhong, K.; Shi, L.; Lu, C.; et al. RPA-CRISPR/cas12a-coupled microfluidic biosensor enabling on-site, sensitive quantification of vibrio parahaemolyticus. *Biosens. Bioelectron.* 2026, *296*, 118327, DOI: 10.1016/j.bios.2025.118327.

(9) Xiao, Y.; Xu, M.; Liao, Z.; Xiong, Y.; Guo, M. A DNA nanoclusters-mediated LAMP/CRISPR-cas12a synergistic amplified biosensor for dual-channel ultrasensitive detection of vibrio parahaemolyticus. *Sens. Actuator B-Chem.* 2026, *460*, 139895, DOI: 10.1016/j.snb.2026.139895.

(10) Xu, H.; Chen, Q.; Meng, X.; Yan, C.; Yao, B.; Chen, Z.; Wang, Z.; Chen, W. CRISPR/cas12a-mediated cyclic signal amplification and electrochemical reporting strategy for rapid and accurate sensing of vibrio parahaemolyticus in aquatic foods. *Biosens. Bioelectron.* 2025, *277*, 117284, DOI: 10.1016/j.bios.2025.117284.

(11) Peng, Y.; Xue, P.; Wang, R.; Shang, H.; Yao, B.; Zheng, Z.; Yan, C.; Chen, W.; Xu, J. Engineering of an adaptive tandem CRISPR/cas12a molecular amplifier permits robust analysis of vibrio parahaemolyticus. *Talanta* 2024, *266*, 125061, DOI: 10.1016/j.talanta.2023.125061.

(12) Wang, J.; Sun, H.; Gao, Y.; Bu, S.; Zhang, Z.; Wang, C.; Zhang, H.; Zhang, W.; Wan, J. A novel biosensor for detecting v. Parahaemolyticus based on cascade signal amplification of CRISPR/cas14a and exo III. *Food Control* 2025, *167*, 110788, DOI: 10.1016/j.foodcont.2024.110788.